

Four-body conversion of atomic helium ions

C. P. de Vries and H. J. Oskam

Department of Electrical Engineering, University of Minnesota, Minneapolis, Minnesota 55455

(Received 24 April 1980)

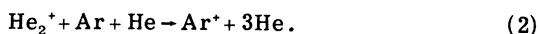
The conversion of atomic helium ions into molecular ions was studied in pure helium and in helium-neon mixtures containing between 0.1 at. % and 50 at. % neon. The experiments showed that the termolecular conversion reaction, $\text{He}^+ + 2\text{He} \rightarrow \text{He}_2^+ + \text{He}$, is augmented by the four-body conversion reaction $\text{He}^+ + 3\text{He} \rightarrow$ products, where the products could include either He_2^+ or He_3^+ ions. Conversion rate coefficients of $(5.7 \pm 0.8) \times 10^{-32} \text{ cm}^6 \text{ sec}^{-1}$ and $(2.6 \pm 0.4) \times 10^{-49} \text{ cm}^7 \text{ sec}^{-1}$ were found for the termolecular and four-body conversion reactions, respectively. In addition, rate coefficients for the following Ne^+ conversion reactions were measured: $\text{Ne}^+ + \text{He} + \text{He} \rightarrow (\text{HeNe})^+ + \text{He}$, $(2.3 \pm 0.1) \times 10^{-32} \text{ cm}^6 \text{ sec}^{-1}$; $\text{Ne}^+ + \text{He} + \text{Ne} \rightarrow (\text{HeNe})^+ + \text{Ne}$ or $\text{Ne}_2^+ + \text{He}$, $(8.0 \pm 0.8) \times 10^{-32} \text{ cm}^6 \text{ sec}^{-1}$; and $\text{Ne}^+ + \text{Ne} + \text{Ne} \rightarrow \text{Ne}_2^+ + \text{Ne}$, $(5.1 \pm 0.3) \times 10^{-32} \text{ cm}^6 \text{ sec}^{-1}$. All rate coefficients are at a gas temperature of 295 K.

I. INTRODUCTION

Recent papers by Lee, Collins, and Waller¹⁻³ have demonstrated that bimolecular (two-body) reactions such as

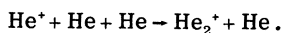


can be significantly augmented by termolecular (three-body) reactions such as

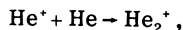


The addition of a helium atom in (2) increases the number of reaction channels and also influences the pressure dependence of the He_2^+ destruction frequency. By measuring this pressure dependence, Lee *et al.*¹ reported rate constants of $2.2 \times 10^{-10} \text{ cm}^3 \text{ sec}^{-1}$ and $2.4 \times 10^{-29} \text{ cm}^6 \text{ sec}^{-1}$ for reactions (1) and (2), respectively. Thus, the termolecular reaction (2) dominates at helium pressures greater than about 300 Torr.

Termolecular reactions have not been studied extensively except for associative reactions, where the number of product species is less than the number of reactants. An example of such a reaction is the conversion of atomic helium ions into molecular helium ions:

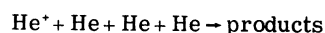


The bimolecular analog to this reaction,



is extremely unlikely from energy and momentum conservation considerations. Therefore, the termolecular reaction dominates even at low helium pressures.

This paper reports evidence that the conversion of atomic helium ions into molecular helium ions is significantly enhanced by the four-body reaction



even at relatively low helium pressures. The conversion rate was measured using standard stationary afterglow techniques applied to mixtures of helium and neon. The addition of neon to the gas allowed measurements of the conversion rate over a wider range than ordinarily possible in pure helium afterglows. Conversion of atomic neon ions was also measured in the experiments, but it did not exhibit any four-body reaction component in the pressure ranges studied.

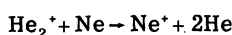
II. EXPERIMENTAL METHOD

The experiments were performed with a differentially pumped quadrupole mass spectrometer system. The spectrometer analyzed the ion wall currents in a cylindrical discharge tube which had a characteristic diffusion length of $0.531 \pm 0.003 \text{ cm}$. The discharge region was defined by a glass cylinder with an inside diameter of 3.21 cm and two planar electrodes 2.76 cm apart. Discharges were produced by high-voltage dc pulses applied between the electrodes. One electrode was made from molybdenum while the other was constructed from a 25 μm thick, 82 at. % Au-18 at. % Ni alloy foil. A 50 μm -diameter hole, located in the center of the foil, served as the sampling orifice.

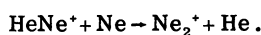
The discharge tube and quadrupole mass spectrometer were part of a standard high-vacuum system which had an ultimate pressure of $2 \times 10^{-9} \text{ Torr}$ after a 24-h bakeout at 320 °C. Helium-neon mixtures were prepared in the vacuum system by volume expansion techniques. Each gas was catalytically purified before mixing. A capacitance manometer measured the gas pressure in the discharge tube and controlled a servo-driven leak valve which compensated for the gas losses

through the sampling orifice.

Ions analyzed by the mass spectrometer were detected by an electron multiplier. The anode pulses from the multiplier were routed through a discriminator and accumulated in a multichannel scalar. The entire detection system was capable of following ion density decays over five orders of magnitude. In helium-neon mixtures containing less than 0.02 at. % neon, He^+ , He_2^+ , HeNe^+ , Ne^+ , and Ne_2^+ ions were observed during the afterglow period. At higher neon concentrations, the He_2^+ and HeNe^+ signals rapidly disappeared due to the bimolecular conversion reactions⁴



and

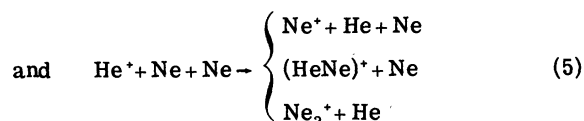
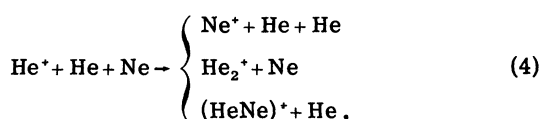
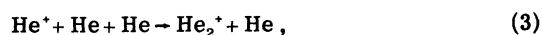


Impurity ion signals were observed at 5, 12, 16, and 28 amu. The signals at 5 and 28 amu can be attributed to $(\text{HeH})^+$ and CO^+ while the signals at 12 and 16 amu can arise from a combination of C^+ , O^+ , He_3^+ , and He_4^+ . In all mixtures, the impurity ion signals, integrated over the afterglow period, were less than 0.05% of the integrated major ion signal.

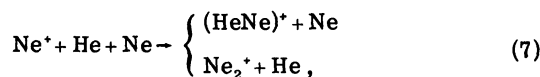
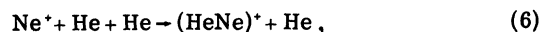
III. AFTERGLOW PROCESSES AND RELEVANT THEORY

The evolution of the He^+ and Ne^+ ion densities in the afterglow can be determined from the continuity equations describing the production and loss processes for each particle. These atomic ions can be lost by ambipolar diffusion, collisional-radiative recombination, and conversion into molecular ions. Diffusion carries the ions to the walls of the discharge region where they are efficiently neutralized and where the ion densities can be assumed to be zero. The influence of volume recombination on the loss rate depends either on the electron density or the square of the electron density and becomes negligible in the later part of the afterglow. Also, the electron temperature is equal to the gas temperature during the later afterglow period.

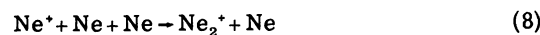
The possible termolecular conversion processes which can occur in helium-neon mixtures are



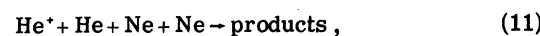
for the atomic helium ion, and



and



for the atomic neon ion. In addition, these atomic ions can be converted by four-body processes, which for He^+ are



and



Here the products have not been shown explicitly but can include He_2^+ , $(\text{HeNe})^+$, Ne_2^+ , and possibly other molecular ions such as He_3^+ .

The solution of the continuity equation describing loss by conversion and diffusion can be written analytically as a sum of modes which decay exponentially at different rates.⁵ The mode with the largest time constant (fundamental mode) dominates in the later part of the afterglow period. Its time constant τ is given by

$$P_0/\tau = D_a P_0/\Lambda^2 + \nu P_0, \quad (13)$$

where P_0 is the reduced gas pressure, D_a is the appropriate ambipolar diffusion coefficient, Λ is the characteristic diffusion length of the plasma container, and ν is the total conversion frequency.

The conversion frequency of atomic helium ions can be expressed as

$$\nu_{\text{He}} = \beta_1 P_0^2 + \beta_2 P_0^3, \quad (14)$$

where

$$\frac{\beta_1}{[3.54 \times 10^{16} \text{ cm}^{-3} \text{ Torr}^{-1}]^2} = k_3 + (k_4 - 2k_3)r + (k_5 - k_4 + k_3)r^2 \quad (15)$$

and

$$\frac{\beta_2}{[3.54 \times 10^{16} \text{ cm}^{-3} \text{ Torr}^{-1}]^3} = k_9 + (k_{10} - 3k_9)r + (k_{11} - 2k_{10} + 3k_9)r^2 + (k_{12} - k_{11} + k_{10} - k_9)r^3, \quad (16)$$

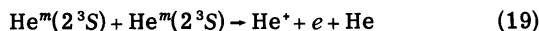
where k_i is the rate coefficient of reaction (i) and $r \equiv [Ne]/([He] + [Ne])$ is the fractional neon concentration. Similarly, excluding possible four-body conversion reactions,

$$\nu_{Ne} = \beta_3 P_0^2 \quad (17)$$

with

$$\frac{\beta_3}{[3.54 \times 10^{16} \text{ cm}^{-3} \text{ Torr}^{-1}]^2} = k_6 + (k_7 - 2k_8)r + (k_8 - k_7 + k_6)r^2. \quad (18)$$

Both atomic helium ions and atomic neon ions can be produced by volume reactions in the afterglow. The metastable-metastable process



is known⁶ to be important in pure helium afterglows, while atomic neon ions can be formed by⁴



When production is included in the continuity equation for an atomic ion, its time dependence becomes a sum of two exponential functions with different time constants. One time constant is given by (13) which describes the loss of the ion, while the other is related to the loss of the reactants which are involved in the production of the ion. The final decay of the ion density will be determined by the largest time constant.

IV. RESULTS

The afterglow time dependencies of the He^+ and Ne^+ number densities were measured as a function of fractional neon concentration and total gas pressure. Both ions were studied in helium-neon mixtures containing 0.1, 0.3, 1, 3, 10, and 50 at. % neon. In addition, each atomic ion was studied in its parent gas. All the experiments were performed at a gas temperature of 295 K.

A. Atomic neon ions

The results obtained for $[\text{Ne}^+]$ in the 0.3 at. % neon mixture are shown in Fig. 1, where the late afterglow decay time constant (expressed as P_0/τ) is plotted versus P_0^3 . At pressures below approximately 4 Torr in Fig. 1, the $[\text{Ne}^+]$ decay is controlled by reaction (20). Above 4 Torr, the data are linear in P_0^3 indicating loss by diffusion and the termolecular conversion reactions (6), (7), and (8). The slope and vertical intercept of the best linear fit to these data give, respectively, the effective termolecular rate coefficient, β_3 , and the ambipolar diffusion coefficient of Ne^+ in the mixture.

The dependence of these quantities on fractional

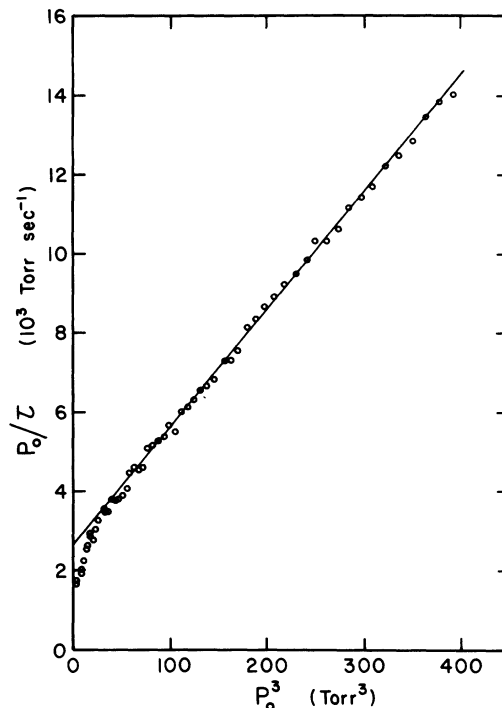


FIG. 1. Measured values of P_0/τ as a function of P_0^3 for the Ne^+ number density in helium containing 0.3 at. % neon. The solid line is the best linear fit to the data above 4.3 Torr.

neon concentration is illustrated in Fig. 2. The reduced Ne^+ mobility, $\mu_{\text{Ne}^+}(r)$, derived from the ambipolar diffusion coefficient in each mixture, obeys Blanc's Law

$$\frac{1}{\mu_{\text{Ne}^+}(r)} = \frac{r}{\mu_{\text{Ne}^+}(1)} + \frac{(1-r)}{\mu_{\text{Ne}^+}(0)}, \quad (21)$$

where $\mu_{\text{Ne}^+}(1)$ and $\mu_{\text{Ne}^+}(0)$ are the reduced mobilities of Ne^+ ions in pure neon and pure helium, respectively. The best linear fit to the data gives values of $\mu_{\text{Ne}^+}(1) = 4.0 \pm 0.1 \text{ cm}^2 \text{ V}^{-1} \text{ sec}^{-1}$ and $\mu_{\text{Ne}^+}(0) = 20.0 \pm 0.5 \text{ cm}^2 \text{ V}^{-1} \text{ sec}^{-1}$ which agree with previously reported results.^{4,7}

From Eq. (18), β_3 varies quadratically in r . The best quadratic fit to the conversion data in Fig. 2 gives values $k_6 = (2.3 \pm 0.1) \times 10^{-32} \text{ cm}^6 \text{ sec}^{-1}$, $k_7 = (8.0 \pm 0.8) \times 10^{-32} \text{ cm}^6 \text{ sec}^{-1}$, and $k_8 = (5.1 \pm 0.3) \times 10^{-32} \text{ cm}^6 \text{ sec}^{-1}$ for the rate coefficients of reactions (6), (7), and (8). The values found for k_6 and k_8 agree with previously reported results^{4,7} while k_7 differs significantly from the value reported by Veatch and Oskam.⁴ This discrepancy can be attributed to the smaller range of neon concentrations used during their studies. Also, they did not take into account the influence of k_6 on the linear term in Eq. (18).

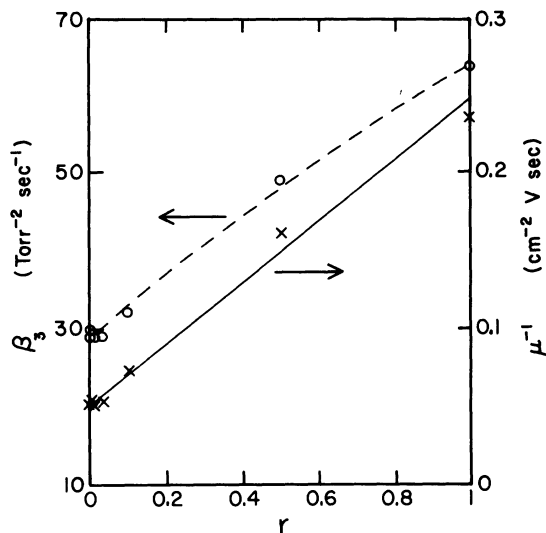


FIG. 2. The inverse mobility (\times) and effective termolecular rate coefficient (\circ) of Ne^+ as a function of fractional neon concentration. The solid line and dashed line are the best linear and quadratic fits to the mobility and rate coefficient data, respectively.

B. Atomic helium ions

The P_0/τ values obtained from the afterglow time dependence of the He^+ density in pure helium are presented in Fig. 3. Below approximately 2 Torr, the time dependence is controlled by diffu-

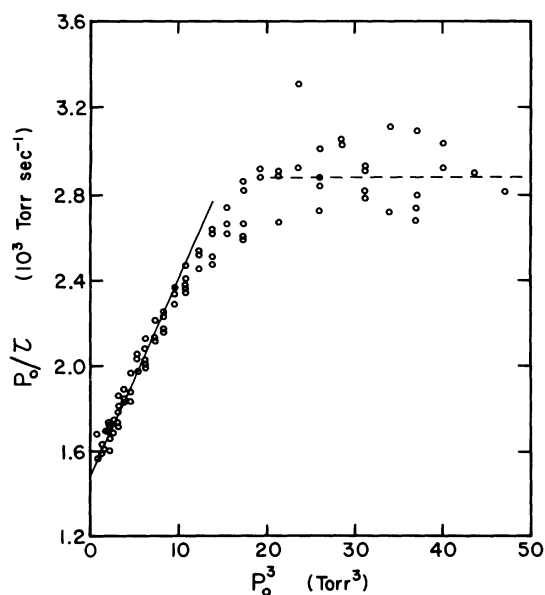
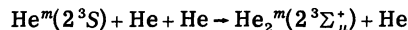


FIG. 3. Measured values of P_0/τ as a function of P_0^3 for the He^+ number density in pure helium. The solid line is the best linear fit to the data below 1.8 Torr. The dashed line represents the average of the data above 2.8 Torr.

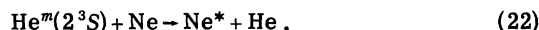
sion and conversion losses. Above 2.8 Torr, the data is determined by the metastable-metastable production of He^+ (19). At the pressures of interest, the $\text{He}^m(2^3\text{S})$ metastable particles are lost mainly by diffusion since the termolecular conversion reaction



has a small rate coefficient.^{8,9} The best fit to the higher pressure data in Fig. 3 (dashed line) yields a value of $D_m P_0 = 410 \pm 15 \text{ cm}^2 \text{ sec}^{-1} \text{ Torr}$ for the diffusion coefficient of the $\text{He}^m(2^3\text{S})$ metastable particle in pure helium. This value is in excellent agreement with measurements using the more direct light absorption technique.⁸⁻¹⁰

As can be seen from Fig. 3, the production process (19) severely limits the pressure range over which the conversion loss of He^+ can be measured in pure helium. Any attempt to determine the He^+ conversion rate coefficient from the data in Fig. 3 must be based on *a priori* assumptions about the pressure dependence of the conversion processes involved. If the termolecular conversion reaction (3) is assumed to dominate, then the best fit to the data below 1.8 Torr (solid line) gives a value of $k_3 = 7.4 \times 10^{-32} \text{ cm}^6 \text{ sec}^{-1}$ which agrees with other reported results obtained under similar conditions.^{6,9,11}

When neon is introduced into the helium gas, the $\text{He}^m(2^3\text{S})$ metastable particles are lost by the excitation transfer reaction¹²



which has a rate coefficient of $k_{22} = 4.3 \times 10^{-12} \text{ cm}^3 \text{ sec}^{-1}$. However, the loss of He^+ ions is not significantly affected by the bimolecular reaction



Fehsenfeld *et al.*¹³ reported an upper limit of $10^{-15} \text{ cm}^3 \text{ sec}^{-1}$ for the rate coefficient of process (23). Thus, the neon selectively reacts with the $\text{He}^m(2^3\text{S})$ metastable particles. The resulting increase in the $[\text{He}^m]$ decay rate extends the pressure range over which the He^+ conversion rate can be measured.

This phenomenon can be observed in Fig. 4 which presents the late afterglow decay time constant (expressed as P_0/τ) of the He^+ density in the 0.3 at. % neon mixture. The dashed line in Fig. 4 indicates the expected P_0/τ pressure dependence if the $[\text{He}^+]$ decay rate was controlled by the metastable-metastable production process (19). However, in this neon mixture, the frequency of process (22) is sufficiently rapid to ensure that the $[\text{He}^+]$ time dependence is controlled by diffusion and conversion losses throughout the pressure range studied.

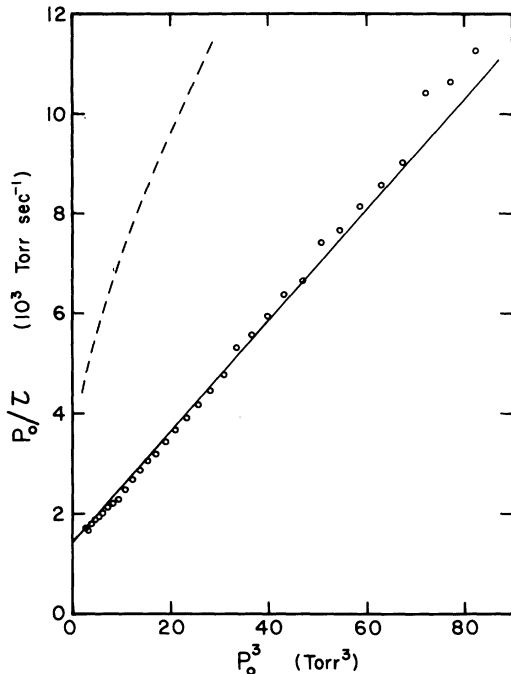


FIG. 4. Measured values of P_0/τ as a function of P_0^3 for the He^+ number density in helium containing 0.3 at. % neon. The solid line is the best linear fit to the data when the vertical intercept is constrained to be $1.43 \times 10^3 \text{ Torr sec}^{-1}$. The dashed line is twice the calculated P_0/τ of the $\text{He}^m(2^3\text{S})$ number density.

The results shown in Fig. 4 are visually linear in P_0^3 . However, the best linear fit to the data yields a vertical intercept of $1290 \text{ Torr sec}^{-1}$ which corresponds to a reduced mobility of $9.4 \text{ cm}^2 \text{ V}^{-1} \text{ sec}^{-1}$ for He^+ . This value is significantly below the accepted value of $10.4 \text{ cm}^2 \text{ V}^{-1} \text{ sec}^{-1}$ in pure helium.^{4,9,14} If the vertical intercept is fixed at a value of $1430 \text{ Torr sec}^{-1}$ [$\mu_{\text{He}^+}(0) = 10.4 \text{ cm}^2 \text{ V}^{-1} \text{ sec}^{-1}$], then the resulting best linear fit (solid line in Fig. 4) overestimates the data at lower pressures and underestimates the data at higher pressures. The variations are small but consistent, and suggest a pressure dependence for P_0/τ of higher order than P_0^3 .

Results similar to Fig. 4 were obtained from each helium-neon mixture containing between 0.1 and 3 at. % neon. In each mixture, the data were best fit by the relation

$$P_0/\tau = D_a P_0/\Lambda^2 + \beta_1 P_0^3 + \beta_2 P_0^4, \quad (24)$$

where β_1 and β_2 describe loss by termolecular conversion and four-body conversion, respectively. The values of $D_a P_0/\Lambda^2$, β_1 , and β_2 determined from these mixtures are presented in Table I. Their consistency indicates that the He^+ conversion rate is due primarily to the pure helium conversion

TABLE I. The values of $D_a P_0/\Lambda^2$, β_1 , and β_2 determined from helium-neon mixtures containing 0.1, 0.3, 1, and 3 at. % neon. Also shown are the values of $D_a P_0/\Lambda^2$ and β_1 obtained from the pure helium results and from the 10 and 50 at. % neon mixtures.

Neon (at. %)	$D_a P_0/\Lambda^2$	β_1	β_2
0	1480	93	
0.1	1360	72	11
0.3	1430	75	10
1	1390	72	13
3	1500	62	13
10	1410	102	
50	1730	66	

reactions (3) and (9) at these lower neon concentrations.

Table I also presents the values of $D_a P_0/\Lambda^2$ and β_1 obtained from the pure helium results (Fig. 3) and from the 10 and 50 at. % neon mixtures. In these cases, the He^+ decay rate could not be measured over a large enough pressure range to separate the influence of termolecular and four-body conversion reactions. Instead, the data were fit without the four-body conversion term in Eq. (24). The reduced mobility of He^+ , derived from $D_a P_0$ in each mixture, obeys Blanc's Law. Values of $\mu_{\text{He}^+}(0) = 10.3 \pm 0.3 \text{ cm}^2 \text{ V}^{-1} \text{ sec}^{-1}$ and $\mu_{\text{He}^+}(1) = 16 \pm 1 \text{ cm}^2 \text{ V}^{-1} \text{ sec}^{-1}$ were obtained for the reduced mobility of He^+ in pure helium and pure neon, respectively.

To better illustrate the contribution of four-body conversion reactions on the $[\text{He}^+]$ decay rate, Eq. (24) can be rewritten as

$$\eta = (P_0/\tau - D_a P_0/\Lambda^2)/P_0^3 = \beta_1 + \beta_2 P_0. \quad (25)$$

Figure 5 presents the values of η obtained from the mixtures containing between 0.1 and 3 at. % neon. In each mixture, the value of $D_a P_0/\Lambda^2$ was calculated from the derived mobility results. As can be seen from Fig. 5, η increases with pressure due to the existence of the four-body conversion rate β_2 . The best linear fit to the data in Fig. 5 (solid line) yields values of $k_3 = (5.7 \pm 0.8) \times 10^{-32} \text{ cm}^6 \text{ sec}^{-1}$ and $k_9 = (2.6 \pm 0.4) \times 10^{-49} \text{ cm}^9 \text{ sec}^{-1}$. These values have been assigned to the pure helium conversion reactions (3) and (9) since the data are essentially identical for the range of neon concentrations covered.

Figure 5 can be compared with Fig. 6 which presents the values of η obtained from the $[\text{Ne}^+]$ decay rate in three helium-neon mixtures. The $[\text{Ne}^+]$ results are constant within experimental error indicating that the Ne^+ conversion rate can be attri-

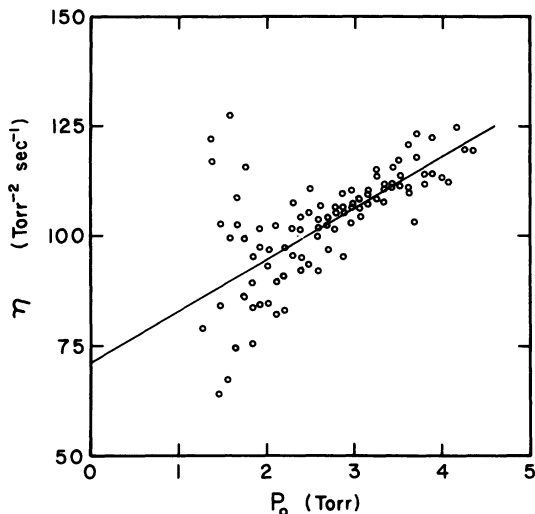


FIG. 5. Measured values of $\eta \equiv (P_0/\tau - D_a P_0/\Lambda^2)/P_0^3$ as a function of gas pressure for the He^+ number density in helium containing 0.1, 0.3, 1, and 3 at.% neon. The solid line is the best linear fit to the data.

buted to the termolecular conversion reactions (6) through (8) in the pressure ranges studied. The comparison between Figs. 5 and 6 is significant because the $[\text{He}^+]$ and $[\text{Ne}^+]$ data were taken simultaneously in each mixture. Any systematic errors which might have led to the results in Fig. 5 should also be apparent in the $[\text{Ne}^+]$ results.

V. DISCUSSION

The pressure dependence of the He^+ conversion frequency shown in Fig. 5 is, to the authors' knowledge, the first reported evidence of a four-body reaction occurring in a gaseous plasma. Its identification at relatively low gas pressures is made possible by the large ratio of k_0 to k_3 . Indeed, the four-body conversion process (9) dominates over the termolecular conversion reaction (3) at helium pressures greater than 6 Torr. This pressure can be contrasted to pressures of 300 Torr and higher used by Lee *et al.*¹⁻³ to measure termolecular reaction rates which parallel bimolecular reaction channels.

The value of $5.7 \times 10^{-32} \text{ cm}^6 \text{ sec}^{-1}$ obtained for k_3 is comparable to the termolecular conversion rates of other atomic rare gas ions.^{4,15-17} However, it is approximately two to three orders of magnitude smaller than the termolecular rates reported by Lee *et al.*¹⁻³ The value of $k_0 = 2.6 \times 10^{-49} \text{ cm}^9 \text{ sec}^{-1}$ cannot be compared with any other four-body reaction rate constant, but its order of magnitude can be justified by the following simplified analysis.

The multibody conversion reactions (3) and (9)

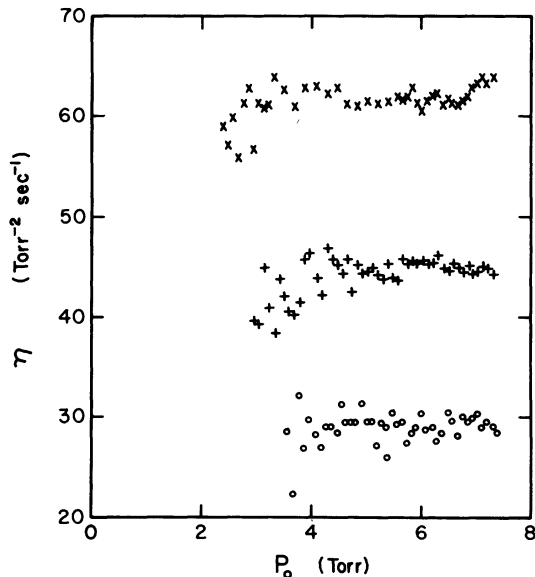
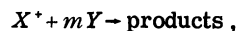


FIG. 6. Measured values of $\eta \equiv (P_0/\tau - D_a P_0/\Lambda^2)/P_0^3$ as a function of gas pressure for the Ne^+ number density in helium containing 0.1 (○), 0.3 (+), and 10 (×) at.% neon. The data from the 0.3 and 10 at.% mixtures have been shifted upward by 15 and 30 $\text{Torr}^{-2} \text{ sec}^{-1}$, respectively.

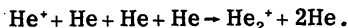
are of the form



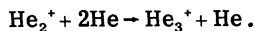
with $m = 1, 2, 3, \dots$. This general multibody process can also be viewed as a two-body reaction between X^+ and a $(Y)_m$ complex. If the latter is defined to exist whenever the m atoms of type Y are within a small volume V , then the density¹⁸ of the complex is $V^{(m-1)}n^m$, where n is the number density of atom Y . The corresponding reaction rate k_m is equal to $\bar{v}\sigma_m V^{(m-1)}$ where \bar{v} is the relative velocity between X^+ and the $(Y)_m$ complex, and σ_m is the effective cross section of the two-body interaction. This estimate indicates that the ratio k_m/k_{m+1} equals V^{-1} , independent of m , provided that the parameters \bar{v} , σ_m , and V are reasonably constant.

Lee *et al.*¹⁻³ reported coefficients on the order of $10^{-9} \text{ cm}^3 \text{ sec}^{-1}$ and $2 \times 10^{-29} \text{ cm}^6 \text{ sec}^{-1}$ for the bimolecular and termolecular reactions between He_2^+ and various reactants. These reaction rates give an approximate value of $V = 2 \times 10^{-20} \text{ cm}^3$ and suggest a four-body rate coefficient of $4 \times 10^{-49} \text{ cm}^9 \text{ sec}^{-1}$. This rough estimate does indicate that the value $k_0 = 2.6 \times 10^{-49} \text{ cm}^9 \text{ sec}^{-1}$ is a realistic value for a four-body rate coefficient.

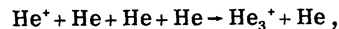
The products of the termolecular conversion reaction (3) are molecular He_2^+ ions and neutral helium atoms. These products can also be formed by the four-body process



Other molecular helium ions are also present in helium afterglows. Both He_3^+ ions and He_4^+ ions have been observed in cryogenic helium afterglows.^{19,20} The He_3^+ ion is generally the dominant ion at gas temperatures below 200 K and is present in small quantities at 300 K.²¹ At this temperature, the He_3^+ ions are in equilibrium with He_2^+ ions according to the relation²¹



The existence of a stable He_3^+ ion suggests that the four-body conversion reaction (9) can also proceed as



where a He_3^+ ion is formed directly.

ACKNOWLEDGMENT

This work was supported by NSF under Grant No. ENG78-25933.

¹F. W. Lee, C. B. Collins, and R. A. Waller, *J. Chem. Phys.* **65**, 1605 (1976).

²F. W. Lee and C. B. Collins, *J. Chem. Phys.* **65**, 5189 (1976).

³C. B. Collins and F. W. Lee, *J. Chem. Phys.* **68**, 1391 (1978).

⁴G. E. Veatch and H. J. Oskam, *Phys. Rev. A* **2**, 1422 (1970).

⁵H. J. Oskam, *Philips Res. Rep.* **13**, 335 (1958).

⁶G. E. Veatch and H. J. Oskam, *Phys. Rev.* **184**, 202 (1969).

⁷A. P. Vitols and H. J. Oskam, *Phys. Rev. A* **5**, 2618 (1972).

⁸A. V. Phelps, *Phys. Rev.* **99**, 1307 (1955).

⁹R. Deloche, P. Monchicourt, M. Cheret, and F. L. Lambert, *Phys. Rev. A* **13**, 1140 (1976).

¹⁰C. P. de Vries and H. J. Oskam, *Phys. Rev. A* **19**, 2095 (1979).

¹¹D. Smith and M. J. Copsey, *J. Phys. B* **1**, 650 (1968).

¹²D. W. Ernie and H. J. Oskam, *Phys. Rev. A* **21**, 95 (1980).

¹³F. C. Fehsenfeld, A. L. Schmeltekopf, P. D. Goldan, H. I. Schiff, and E. E. Ferguson, *J. Chem. Phys.* **44**, 4087 (1966).

¹⁴R. Johnsen, M. T. Leu, and M. A. Biondi, *Phys. Rev. A* **8**, 2557 (1973).

¹⁵D. Smith and P. R. Cromey, *J. Phys. B* **1**, 638 (1968).

¹⁶C. J. Tracy and H. J. Oskam, *J. Chem. Phys.* **65**, 3387 (1976).

¹⁷A. P. Vitols and H. J. Oskam, *Phys. Rev. A* **8**, 1860 (1973).

¹⁸For an ideal gas of density n , the probability of finding one particle in a small volume V is Vn . The probability of finding m particles in a small volume is $V^m n^m$. The corresponding density is the probability divided by V .

¹⁹C. P. de Vries and H. J. Oskam, *Phys. Lett.* **29A**, 299 (1969).

²⁰R. A. Gerber and M. A. Gusinow, *Phys. Rev. A* **4**, 2027 (1971).

²¹M. A. Gusinow, R. A. Gerber, and J. B. Gerardo, *Phys. Rev. Lett.* **25**, 1248 (1970).